1-2020

Astrocytic response to neural injury is larger during development than in adulthood and is not predicated upon the presence of microglia

Andrew J. Riquier

Suzanne I. Sollars

Brain, Behavior, & Immunity - Health 1 (2020) 100010

Contents lists available at ScienceDirect

Brain, Behavior, & Immunity - Health

journal homepage: www.editorialmanager.com/bbih/default.aspx

Full Length Article

Astrocytic response to neural injury is larger during development than in adulthood and is not predicated upon the presence of microglia

Andrew J. Riquier, Suzanne I. Sollars *

University of Nebraska at Omaha, 6001 Dodge Street, Omaha, NE, 68182, USA

ARTICLE INFO

Keywords:
PLX5622
Colony-stimulating factor 1 receptor inhibitor
Chorda tympani
Gustatory
Nerve transection

ABSTRACT

While contributions of microglia and astrocytes are regularly studied in various injury models, how these contributions differ across development remains less clear. We previously demonstrated developmental differences in microglial profiles across development in an injury model of the gustatory system. Nerves of the rat gustatory system have limited capacity to regenerate if injured during neonatal ages but show robust recovery if the injury occurs in adulthood. Using this developmentally disparate model of regenerative capacity, we quantified microglia and astrocytes in the rostral nucleus of the solitary tract (rNTS) following transection of the gustatory chorda tympani nerve (CTX) of neonatal and adult rats. We found that neonatal CTX induced an attenuated microglia response but a larger astrocyte response compared to adult CTX. To elucidate the interplay between the microglia and astrocyte responses in the CTX model, we used our novel intraperitoneal injection protocol for the colony-stimulating factor 1 receptor inhibitor PLX5622 to deplete microglia in the neonatal and adult rat brain prior to and after CTX. PLX5622 depleted microglia by 80–90% within 3 days of treatment, which increased to > 90% by 7 days. After 14 days of PLX5622 treatment, microglia were depleted by > 96% in both neonates and adults while preserving baseline astrocyte quantity. Microglia depletion eliminated the adult astrocyte response to CTX, while the neonatal astrocyte response after injury remained robust. Our results show injecting PLX5622 is a viable means to deplete microglia in neonatal and adult rats and suggest developmentally distinct mechanisms for astrogliosis following neural injury.

1. Introduction

The profound malleability of the developing nervous system can be both facilitating (Himes and Tessler, 1989; Villablanca et al., 1986) and detrimental (Kolb et al., 1987; Omelian et al., 2016; Sollars, 2005; Taylor and Alden, 1997) to injury recovery. Such plasticity is facilitated in part by microglia and astrocytes, omnipresent co-functioning innate immune glial cells of the central nervous system. Microglia and astrocytes increase in number, assume a reactive morphology, as well as upregulate and secrete pro and anti-inflammatory cytokines following central nervous system injury (Bylicky et al., 2018; Gao et al., 2013; Sofroniew, 2014), inflammation induction (Liddelow et al., 2017; Smith et al., 2014), and disease (Heneka et al., 2015; Stephenson et al., 2018). Comparable responses are induced in the central terminals or around the centrally located cell bodies of axotomized peripheral nerves such as the sciatic nerve (Hu et al., 2007), infraorbital nerve (Melzer et al., 2001), facial motor neurons (Graeber et al., 1998; Tyzack et al., 2014). Differences in the magnitude, function, and inflammatory profiles of microglia and astrocytes following injury are associated with differences in primary and secondary damage (Cherry et al., 2014; Tang and Le, 2016) and recovery outcomes (Liddelow et al., 2017; Pekny and Pekna, 2014) and appear to vary based on developmental stage (Goranova et al., 2009; Melzer et al., 2001).

A useful model with which to study the interaction between developmental differences in glia responses and injury recovery is that of the chorda tympani transection (CTX). The chorda tympani (CT) innervates fungiform and a small subset of foliate taste buds on the tongue, transmitting gustatory information to the rostral nucleus of the solitary tract (rNTS) of the brainstem. Fifty days after neonatal (≤ 10 days of age; ≤ P10) CTX fungiform taste buds and CT fibers in the rNTS are almost completely absent (Martin et al., 2019; Sollars, 2005). This lack of recovery is associated with a subdued yet significant microglia response in the central CT fibers in the rNTS (Riquier and Sollars, 2017). CTX in adulthood (> P40), in contrast, has no such long-term effects as recovery is nearly complete (Kopka et al., 2000; Reddaway et al., 2012; St. John et al., 1995) and corresponds with a robust microglia and astrocyte

* Corresponding author.
E-mail address: ssollars@unomaha.edu (S.I. Sollars).

https://doi.org/10.1016/j.bbih.2019.100010
Received 30 September 2019; Received in revised form 15 October 2019; Accepted 18 October 2019
Available online xxxx

response (Bartel, 2012; Bartel and Finger, 2013; Riquier and Sollars, 2017). The developmental difference in the microglia response may be due to the higher baseline inflammatory profile and phagocytic nature (Crain et al., 2013; Hammond et al., 2019; Li et al., 2019) and quantity (Nikodemova et al., 2015; Riquier and Sollars, 2017) of microglia in the early postnatal brain. Microglia genotype and inflammatory profile can in turn drive astrocyte reactivity and function, both promoting (Bylicky et al., 2018; Shinozaki et al., 2017) and inhibiting (Liddelow et al., 2017) injury recovery. However, the astrocyte response to neonatal CTX has yet to be assessed.

Microglia viability is dependent on the receptor tyrosine kinase colony-stimulating factor 1 receptor (CSF1R; Elmore et al., 2014). When integrated into rodent food, CSF1R inhibitors such as PLX3397 and PLX5622 (Plexxikon Inc.) results in > 97% depletion of microglia in mice while maintaining animal health and peripheral monocyte/macrophage quantities (e.g. Elmore et al., 2018; Elmore et al., 2015; Elmore et al., 2014; Hilla et al., 2017; Waisman et al., 2015). Such methods of microglia depletion have been used in several mouse models such as hippocampal neural loss (Rice et al., 2015), optic nerve injury (Hilla et al., 2017), sciatic nerve ligation (Lee et al., 2018), postoperative cognitive decline (Feng et al., 2017) and numerous neurological disorders (Reviewed in Han et al., 2018). However, consumption-based PLX3397 and PLX5622 administration does not provide comparable microglia depletion in rats. Use of food-based drug delivery severely limits the drug application in preweaning animals. While PLX5622-integrated chow consumed by a mouse dam depletes microglia in embryonic and preweaning animals, this indirect administration results in reduced litter size, increased early postnatal mortality and health deficits in surviving pups (Rosin et al., 2018). In the current study, we developed a novel protocol of intraperitoneal administration PLX5622 to deplete microglia in both the early postnatal and adult rat brain. We subsequently quantified the microglia and astrocyte presence in the rNTS during normal development and following neonatal or adult CTX, using PLX5622 to determine the necessity of microglia for astrogliosis in the CTX paradigm.

2. Materials and methods

2.1. Subjects

Male and female Sprague Dawley rats ($n = 72$) bred in the University of Nebraska at Omaha Vivarium were used, with date of birth being denoted as P0 (postnatal day 0). A rat model was selected to correspond with our previous work demonstrating differences in recovery and microglia responses between CTX occurring in adult or neonatal rats (Martin et al., 2019; Riquier and Sollars, 2017; Sollars, 2005). Every condition included both male and female rats randomly assigned from at least two litters. Rats were kept on a 12:12 light-dark cycle in clear Plexiglas cages with free access to tap water and food pellets (Teklad). Rats were weaned at P25 and socially housed. All procedures were carried out in accordance with the National Institutes of Health guide for the care and use of Laboratory animals (NIH Publications No. 8023, revised 1978) and were approved by the local Institutional Animal Care and Use Committee.

2.2. Chorda tympani transection

Rats underwent chorda tympani transection at either P10 ($n = 31$) or P50 ($n = 27$) as previously described (Martin et al., 2019; Riquier and Sollars, 2017; Sollars, 2005). Briefly, after anesthetization with methohexital sodium (60 mg/kg i.p.), the right CT was accessed through an incision in the ventromedial neck, crushed, and the CT was evulsed. Animals were then placed on a heating pad until recovery. The left CT remained intact to serve as an internal sham surgery control. While using the sham side as a control is common following CTX (e.g. Bartel and Finger, 2013; Riquier and Sollars, 2017; Sollars, 2005), there is some evidence of contralateral alternations to electrophysiological nerve activity (Martin and Sollars, 2015; Wall and McCluskey, 2008) and taste bud volume (Guagliardo and Hill, 2007; Li et al., 2015). To validate the sham side as a control, sham-side microglia and astrocyte densities were compared to age-matched intact, non-surgical animals.

2.3. Microglia inhibition via intraperitoneal injection of PLX5622

Prior CSF1R inhibitor studies using PLX3397/5622-integrated chow treated animals for at least 1 week prior to their experimental manipulation (e.g. Elmore et al., 2014; Okunukia et al., 2019). To ensure adequate microglia depletion for neonatal surgeries, we began our treatments at P1, with an equivalent pre-surgery treatment duration (9 days) for adults. Pilot testing indicated that while a single daily injection of 0.65% PLX5622 suspended in 5% dimethyl sulfoxide and 20% Kolliphor RH40 in 0.01 M PBS was sufficient for neonatal microglia depletion, adult depletion required injections twice daily (10–12 h apart). Starting at P1 (for P10 CTX) or P41 (for P50 CTX), additional rats were injected with either PLX5622 (50 mg/kg; $n = 4$–5/condition) or a vehicle solution ($n = 3$–4/condition) once (neonates) or twice (adult) a day until being sacrificed 4 days after surgery.

2.4. Perfusion and tissue extraction

Following anesthesia with a mixture of ketamine/xylazine at 4 days post-CTX, rats were transcardially perfused with a modified Krebs solution (pH 7.3) followed by 4% paraformaldehyde. Brains were extracted and post-fixed overnight in 4% paraformaldehyde at 4 °C. Brainstems were sectioned horizontally at 40 μm on a vibrating microtome, consistent with previous work (Martin et al., 2019; Riquier and Sollars, 2017).

2.5. Immunohistochemistry

Alternating free-floating sections were stained for either microglia or astrocytes with antibodies against Iba1 or GFAP, respectively. To test for microglia phagocytic capacity, separate brains were processed using an antibody against CD68. For all antibodies, 0.01 M PBS (pH 7.4) was used for all solutions and rinses unless otherwise specified. For each immunohistochemistry (IHC) run, between 6 and 8 brains of mixed conditions were processed simultaneously to mitigate any potential influence of inter-run chromogen variability. Spleen tissue was used as a positive control for CD68 due to the high quantity of resident CD68 $^{+}$ cells (Olsson et al., 2012; company data sheet). Brain (Iba1 and GFAP) and spleen (CD68) sections were processed with the primary antibodies omitted as negative controls. No staining was observed on any negative control sections (see Fig. 1 for photomicrographs of control spleen sections).

2.6. Primary antibodies

Ionized calcium-binding adapter molecule 1 (Iba1). A common microglia marker (Bartel, 2012; Bartel and Finger, 2013; Riquier and Sollars, 2017), Iba1 expression is specific to microglia/macrophages

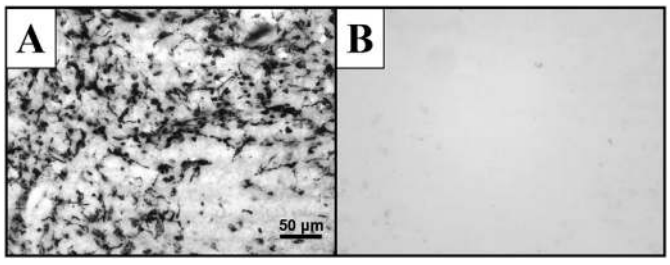

Fig. 1. Control spleen sections for immunohistochemistry controls with (A) the full protocol and (B) omitting the primary antibody. While no CD68 was observed in negative control sections, all positive control sections displayed robust CD68 staining.

(Imai et al., 1996; Ito et al., 1998). After rinsing 3 times for 10 min each, sections were blocked against endogenous peroxidase for 30 min in 0.3% H2O2 in methanol, followed by another rinse cycle. Tissue was blocked against non-specific binding in 2% normal goat serum (NGS), 1% BSA, and 0.3% Triton X-100 for 1 h at room temperature, then incubated with a rabbit anti-Iba1 antibody (1:10,000, Wako, Cat # 019–19741, RRID: AB_839504) in the blocking solution for 36–48 h at 4° Celsius.

Cluster of differentiation 68 (CD68). CD68 is a scavenger receptor commonly expressed on monocytic cells that facilitates clearage of cellular debris via phagocytosis (Suzuki et al., 2014; Zabel et al., 2016) and can be upregulated on microglia following injury (e.g. Goranova et al., 2015; Graeber et al., 1998). Sections were rinsed twice for 5-min each in tris buffered saline (TBS; pH 7.6) containing 0.025% Triton 100-X, followed by blocking for 2 h in TBS containing 10% NGS and 1% BSA at room temperature. Overnight incubation at 4° Celsius with a rabbit anti-CD68 antibody (1:500 in 1% BSA in TBS, Abcam, Cat # ab125212, RRID: AB_10975465) followed. Tissue was then rinsed and placed in the 0.3% H2O2 in methanol for 30 min.

Glial fibrillary acid protein (GFAP). Part of an intermediate filament protein family, GFAP is upregulated following injury and is necessary for astrogliosis (Reviewed in Sofroniew and Vinters, 2010). Thus, any astrocytes that are reacting to CTX will be detectable with an antibody against GFAP. Sections were rinsed 5 times for 5 min each in PBS containing 0.2% Triton 100-X, were blocked for 90 min in 5% NGS, then incubated in a rabbit anti-GFAP antibody (1:13,000, Abcam, Cat # ab7260, RRID: AB_305808) solution containing 5% NGS overnight 4° Celsius. Sections were then rinsed and blocked in 0.3% H2O2 in methanol for 30 min.

2.7. Secondary antibody and visualization

All sections were rinsed 3 times for 10 min each in PBS, then incubated with a goat-anti-rabbit antibody (Vector Laboratories, Cat # BA-1000, RRID: AB_2313606, 1:1000 in 2% NGS, 0.3% Triton X-100) for 2 h at room temperature. Following a rinse cycle, sections were placed in the 2% avidin-biotin complex solution containing 0.1% Triton X-100 (Vector Laboratories, Burlingame, CA) for 1 h, rinsed, then placed in a diaminobenzidine solution (0.05% with 0.125% nickel ammonium sulfate and 0.01% H2O2). The nickel was omitted from GFAP sections, which were counterstained with 1% cresyl violet.

2.8. NTS identification

All visualization and quantification was performed with a brightfield microscope, with the NTS being visualized using phase-contrast (Martin et al., 2019). The most prominent landmarks of the NTS are located on approximately 4 sections (160 μm) halfway through its dorsal-ventral extent, which consist of the solitary tract being visible in the medial NTS across the rostral/caudal plane and prominent facial nuclei rostral to the NTS. Data was collected from these 4 sections, as well as 160 μm dorsally and ventrally, for a total of 12 sections (480 μm), as we have done previously (Riquier and Sollars, 2017). Because the CT terminal field occupies the rostral most $^{1}/_{3}$ of the NTS (Corson and Hill, 2011), this area was identified and traced using a 250 μm × 250 μm square grid projected onto the tissue using the software Neurolucida software (MBF Bioscience, https://www.mbfbioscience.com, RRID:SCR_001775) as we have done previously (Riquier and Sollars, 2017).

2.9. Cell quantification and correction

All cells were visualized using a 20× (1.6) objective lens and were quantified by placing Neurolucida overlay markers on each cell body (microglia and CD68) or cresyl violet stained GFAP + cell (astrocytes). Cells were counted by trained, blind researchers on alternating sections for each cell type and were only counted if the soma was entirely within the outlined rNTS. Markers were totaled using the companion software NeuroExplorer. To mitigate any potential overcounting, an Abercrombie correction (Abercrombie, 1946) was performed using the following formula: Corrected Counts = Raw Counts * (section thickness/[section thickness + cell height]). Cell heights were determined by carefully measuring the soma diameter of a random sampling (~5%) of microglia and astrocytes from control animals of each age, generating a single mean value each for microglia and astrocyte height.

2.10. Data analysis

All analyses were conducted using SPSS Statistics 24 (IBM). Density of cells in the rNTS were used for all analyses to facilitate comparisons across age conditions and varying rNTS sizes. The volume of each rNTS side (right or left) for each animal was calculated by summing the total traced area on each side and multiplying those values by the section thickness (40 μm). Raw cell counts for each antibody were summed to obtain a single value for each rNTS side per animal. These totals were then divided by the respective rNTS volumes and multiplied by 200,000 to get the density of cells (number of cells/200,000 μm^3).

The efficacy of PLX5622-driven microglia depletion was determined using independent samples t-tests comparing sham sides of PLX5622 treated animals to the sham sides of Vehicle treated animals. Due to previous PLX5622 administration during development resulting in abnormal weight gain in mouse pups (Rosin et al., 2018), weights were compared between PLX5622 and vehicle-treated neonatal rats for each day of treatment using independent samples t-tests. These weights were also used to ensure pup health.

The effect of CTX on microglia and astrocyte densities in the rNTS was determined using a 2 (Surgical Side [Sham vs. CTX]) X 2 (Surgical Age [P10 vs P50]) repeated measures ANOVA. Post-hoc analyses were performed using paired-samples t-tests comparing sham sides to CTX sides within each surgical age. To test for contralateral effects of CTX on microglia and astrocyte densities, independent samples t-tests were used to compare the sham side of surgical animals to densities from age-matched intact, non-surgical animals. For ANOVAs, Mauchly's Test of Sphericity was performed to ensure the sphericity assumption was not violated.

Microglia density is highest in the developing rNTS (Riquier and Sollars, 2017), whereas astrocyte quantity increases in other brainstem regions during the first 3 weeks of life (Bandeira et al., 2009). Therefore, direct comparisons of raw condition means across age may mask certain effects. To account for this, the percent increase from baseline cell density between transected and sham sides for each animal was calculated using the formula: [{(transected side density/intact side density) * 100} − 100]. Independent samples t-tests were used to compare the percent of change in microglia and astrocyte density between surgical ages within each days-post condition.

3. Results

3.1. I.P. Injection of PLX5622 severely depletes microglia in developing and adult rats without impacting astrocyte densities

Animals were treated with PLX5622 or vehicle starting nine days prior to surgery (P1 or P41). To assess the timing of microglia depletion, two adult and two neonatal rats were sacrificed after 3 days of PLX5622 administration, and we observed 80% and 90% (± 4%) microglia depletion in the brainstem, respectively. Two additional adult and neonatal rats were sacrificed after 7 days of treatment, and microglia loss had increased to 93% (± 1%) for both ages. The remaining brains were collected 4 days after surgery, for a total of 14 days of treatment. The weights of rat pups did not differ between PLX5622 and vehicle treated neonates (*ps* > .1; Fig. 2) and were consistent with previous reports on rat pup weights (Bandeira et al., 2009) indicating that drug treatment did not impact normal pup health or growth.

Microglia densities did not differ on the intact sides of vehicle and

untreated animals at P14 t (7) = 0.265, p = .768, or P54 t (8) = −0.973, p = .359, indicating that the vehicle had no impact on microglia density. Relative to vehicle-treated animals, 14 days of i.p. PLX5622 injections reduced microglia density in both neonates (96% loss; t (6) = −23.576, p < .001, d = 16.67) and adults (99% loss; t (6) = −10.567, p < .001, d = 7.47; Fig. 2). This loss is comparable or greater than that of administration via food (Elmore et al., 2018; Hilla et al., 2017), and oral gavage (Lee et al., 2018).

Relative to P54 untreated animals, neither the PLX t (7) = 1.527, p = .171 nor Vehicle treatments t (5) = 2.157, p = .08, d = 0.34 influenced astrocyte density on the intact side. This held true for P14 animals treated with PLX t (6) = 0.466, p = .658 or Vehicle t (6) = 0.476, p = .651 relative to untreated animals. Therefore, regardless of age, neither vehicle treatments nor microglia depletion using PLX5622 impacted baseline astrocyte density, in contrast to other i.p. microglia depletion methods such as liposome-encapsulated clodronate intraperitoneal microglia depletion (Han et al., 2019).

3.2. There is a larger microglia response to adult CTX

Because astrocyte and microglia densities on both the intact and transected sides did not differ between untreated and vehicle-treated animals (*ps* > .1), these values were combined for analyses. Four days after CTX there was a significant main effect of surgery on microglia density F (1, 17) = 195.004, p < .001. The main effect of age was also significant F (1, 17) = 4.549, p = .048, as was the interaction between surgery and age F (1, 17) = 6.345, p = .022, suggesting that the effect of surgery differed across surgical age. T-tests revealed that consistent with previous work (Nikodemova et al., 2015; Riquier and Sollars, 2017) baseline microglia densities were highest during early development t (19) = 4.978, p < .001, d = 2.13. Microglia density increased on the transected side after both P10 t (8) = 8.632, p < .001, d = 3.42 and P50 t (9) = 11.183, p < .001, d = 3.37 CTX (Fig. 3A–E). While the percent increase from control levels was larger after P50 CTX t (17) = 4.075, p = .001, d = 1.89 (Fig. 3F), microglia density on the transected side did not differ between P10 and P50 CTX t (17) = 0.630, p = .537. No CD68 was detected at either surgical age.

3.3. The neonatal astrocyte response is larger than adults'

Consistent with previous work (Taft et al., 2005), astrocytes did not differ overall across age F (1, 13) = 1.619, p = .225. However, there was a significant main effect of surgery on astrocyte density F (1, 13) = 50.643, p < .001 and the interaction between surgery and age was significant F (1, 13) = 20.339, p = .001, indicating that the astrocyte increase following CTX differed across age. Indeed, t-tests revealed that although astrocytes increased on the transected side at both P10 t (7) = 6.491, p < .001, d = 2.12 and P50 t (6) = 4.443, p = .004, d = 1.73 (Fig. 3G–K), the percent increase was significantly larger at P10 t (13) = 3.322, p = .006, d = 1.78 (Fig. 3L).

3.4. Microglia are required for the astrocyte response to CTX in adults but not neonates

Similar to untreated animals, P10 CTX induced a significant increase in astrocyte density on the transected side of PLX5622-treated animals t (3) = 6.282, p = .008, d = 4.01. The magnitude of the increase was not affected by PLX5622 treatment t (10) = 1.292, p = .225, suggesting the astrocyte response to P10 CTX is not dependent on microglia. However, microglia depletion using PLX5622 abolished the astrocyte response to

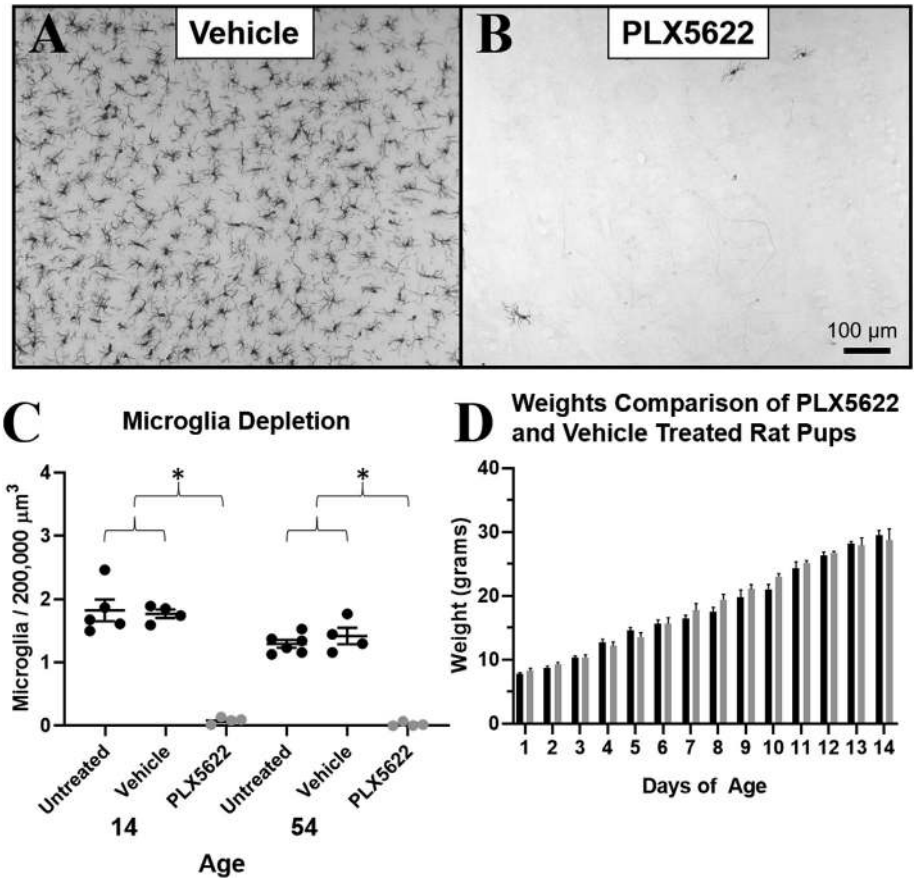

Fig. 2. Compared to vehicle-treated animals (A), intraperitoneal injection of PLX5622 (B) depletes microglia in the neonatal and adult rat NTS (C). (D) Weights of PLX5622 and vehicle treated pups did not differ. Scale bar is 100 µm. Lines (C) and bars (D) denote means ± SEM.*p < .001.

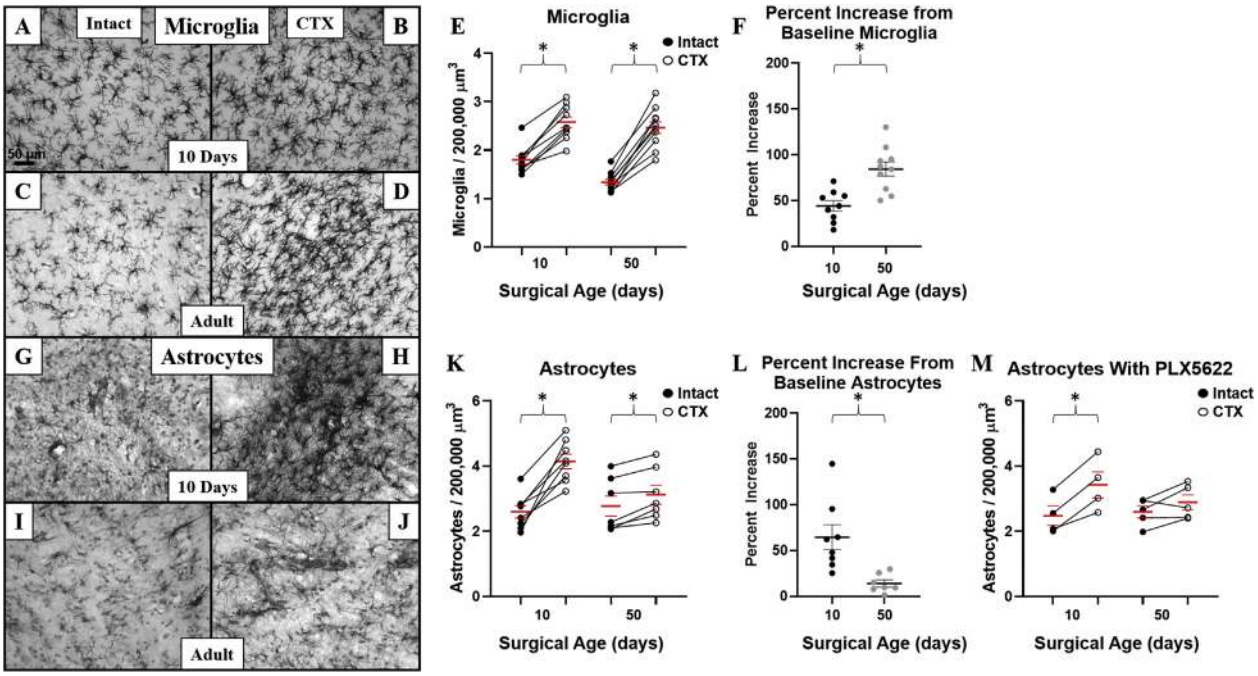

Fig. 3. Microglia (A–F) and astrocytes (G–L) in the intact (A, C, G, I) and transected (B, D, H, J) rNTS 4 days after CTX. While both cell types increase in quantity regardless of surgical age (E, K), surgery at postnatal day 10 induced a smaller microglia (F) and a larger astrocyte (L) response than surgery at postnatal day 50. Microglia depletion with PLX5622 has no effect on the neonatal astrocyte response to CTX but eliminates the adult astrocyte response (M). Each point represents data from a single animal. Connecting lines (E, K, M) show paired comparisons within a single animal. Error bars denote means ± SEM. *$p < .05$. Scale bar is 50 µm.

P50 CTX $t\ (4) = 1.699$, $p = .165$, $d = 0.70$ (Fig. 3M). This indicates that microglia are required for the astrocyte response to P50 CTX.

4. Discussion

In the current study, we provide evidence of developmental differences in both the magnitude and microglia-dependency of NTS astrocytes following CTX. We also demonstrate that i.p. injection of the colony-stimulating factor receptor 1 antagonist PLX5622 ablates microglia from the developing and adult rat brain yet has no impact on baseline astrocyte quantities. While CTX induced an increase in both glia types in the rNTS, the nature of the response differed developmentally. While the microglia response to adult CTX was larger than that of neonates, the astrocyte response was largest in neonates. Further, microglia depletion eliminated the astrocyte response to adult CTX, yet the neonatal astrocyte response was unaffected.

4.1. Developmental difference in the glia response in the injured rNTS

Consistent with our previous work, microglia density increased in the rNTS following ipsilateral CTX, independent of surgical age, although a much greater increase was observed in adults (Riquier and Sollars, 2017). The larger adult response is likely driven by the higher baseline microglia density observed neonatally. Further, as the microglia densities on the surgical side of both age conditions were equivalent, it is possible that there is a ceiling effect on rNTS microglia density. The increase in microglia density is likely due primarily to local proliferation with limited migration as is seen following adult mouse CTX (Bartel, 2012) and whole facial nerve axotomy (Tay et al., 2017). We further observed an increase in astrocytes in the ipsilateral rNTS four days following both adult and neonatal rat CTX, consistent with observations in the adult mouse (Bartel, 2012; Bartel and Finger, 2013). However, while the astrocyte response to adult rat CTX was a modest 13% increase, the increase in the neonatal brain was a substantially larger 64%. This increase was not due to differences in baseline astrocyte values. An increase in astrocyte quantity is commonly preceded by a microglia response which can trigger pathway-dependent differences in reactive astrocyte function (Liddelow et al., 2017; Shinozaki et al., 2017).

It is possible that the increased astrocyte response observed following neonatal CTX is due to the degree of CT fiber loss post-CTX. Neonatal CTX results in substantial CT fiber loss in the NTS 50 days later (Martin et al., 2019), while adult CTX has minimal fiber loss (Reddaway et al., 2012). Although the onset of CT fiber degeneration in neonatal rats has not been established, in adult hamsters, limited CT fiber degeneration begins 2 days after CTX (Whitehead et al., 1995), corresponding with loss of innervated taste buds on the tongue (Sollars, 2005). Unlike in the degenerating facial motor nucleus after facial nerve axotomy (Graeber et al., 1998), rNTS microglia in the CTX paradigm do not express CD68 4-days post CTX, indicating a lack of phagocytic capacity. However neonatal CTX-induced taste bud loss is not observed until a week after CTX (Sollars, 2005), suggesting that CT denervation may be delayed. Future research is therefore needed to see if microglia acquire the ability to phagocytose at a later point. It is also possible that phagocytosis of degenerating CT fibers is performed by astrocytes, as in the CTX paradigm more astrocytes corresponds to greater CT fiber loss (Martin et al., 2019). Damaged fibers can release ATP which can induce astrocyte reactivity (Burda et al., 2016). Indeed, the lack of $CD68^+$ microglia following CTX at either developmental stage suggests that perhaps astrocytes, which phagocytose via ATP-binding cassette transporter A1 (Morizawa et al., 2018), are responsible for phagocytosing debris following CTX, although this hypothesis necessitates further study.

4.2. Developmental difference in necessity of microglia for induction of astrocyte response

We observed that preventing the substantial microglia response to adult CTX consequently prevented an astrocyte increase. Comparable microglia depletion occurring in neonatal rats had no impact on the astrocyte response to CTX, suggesting developmental differences in the mechanisms of CTX-induced astrogliosis. While we cannot eliminate the possibility that the remaining 4% of microglia in the neonatal brain were sufficient to induce an astrocyte response of comparable magnitude and

timeliness as microglia-replete animals, this possibility seems unlikely. The modest microglia increase following neonatal CTX occurs concurrently with a substantial astrocyte response, suggesting an independent, or at least additive, means of astrocyte activation.

While astrocytes can promote injury recovery (Pekny and Pekna, 2014), inflammatory cytokines such as tumor necrosis factor α can induce A1 astrocyte activation, which are deleterious to recovery (Liddelow et al., 2017). The milieu of the developing brain is inherently more inflammatory than that of the adult brain (Crain et al., 2013) which, coupled with the larger neonatal astrocyte response may contribute to the lack of recovery observed following neonatal CTX. However, since microglia are canonically a primary source of neuroinflammation in the developing brain, their absence via PLX5622 treatment likely attenuates the baseline inflammatory profile of the brain. Further research is needed to test the possibility that while the post-CTX astrocyte quantities are comparable between PLX5622 treated and control animals, reduced neuroinflammation may alter astrocyte function.

We observed neither increased mortality nor abnormal weight changes when starting PLX5622 treatments at postnatal day 1 in rats. A recent study provided PLX5622 in food to pregnant mouse dams as a method of depleting microglia in the fetuses. The dams' consumption of the food started at post-conception day 3.5 (E3.5) and resulted in successful depletion of microglia by $>$ 99% in the fetal mice by E15.5. Despite treatment cessation causing postnatal microglia repletion, depletion during this prenatal period resulted in decreased litter size, as well as increased apoptotic cells, decreased neurons, and abnormal weight gain relative to controls by postnatal day 5 (Rosin et al., 2018). The timing of PLX5622 administration is likely a substantial reason for the differences in pup viability we found. Microglia migrate into the CNS at E10.5 in mice (Ginhoux et al., 2010). Microglia depletion during this period appears to disrupt critical stages of embryonic neural development, yet postnatal development demonstrates resiliency to microglia loss.

5. Conclusions

In summary, we demonstrated glial responses to CTX that varied based on developmental stage. Adult CTX induces large microglia and small astrocyte responses, but CTX at P10 results in small microglia and large astrocyte responses, which are associated with differences in CTX recovery (Kopka et al., 2000; Martin et al., 2019; Reddaway et al., 2012; Sollars, 2005; St. John et al., 1995). We are the first to demonstrate that i.p. administration of PLX5622 to both early postnatal and adult rats depletes microglia without impacting animal health (as assessed by weight) or astrocyte quantity. While such depletion eliminated the adult astrocyte response, the neonatal response appeared unaffected, showing that microglia are likely not required for neonatal CTX-induced astrogliosis. Our findings suggest the presence of pathway-specific developmental differences which may contribute to differences in recovery across development. Our results add to existing knowledge regarding differences in glia function across development and factors that may contribute to why the developing gustatory system has difficulty recovering from injury. Our findings highlight the potential importance of central glia to both the developing and injured gustatory system and suggest differences in reciprocal interactions between microglia and astrocytes across maturational stages.

Data availability statement

The data used for this paper are available from the corresponding author upon reasonable request.

Declaration of competing interest

The authors have no competing interests nor conflicts of interest to disclose.

Acknowledgements

This work was supported by the National Institutes of Health [DC04846], the Buffett Early Childhood Institute, and the University of Nebraska at Omaha Office of Research and Creative Activity. PLX5622 powder and ongoing technical support were provided under a Material Transfer Agreement with Plexxikon Inc. These organizations did not influence the study design nor data acquisition and interpretation. The authors thank Afrah Rasheed for assistance with microglia quantification, and Louis Martin, Kristi Apa, Jonathon Hollingsworth, and Blake Andersen for comments on an earlier version of this manuscript.

References

Abercrombie, M., 1946. Estimation of nuclear population from microtome sections. Anat. Rec. 94 (2), 239–247. https://doi.org/10.1002/ar.1090940210.

Bandeira, F., Lent, R., Herculano-Houzel, S., 2009. Changing numbers of neuronal and non-neuronal cells underlie postnatal brain growth in the rat. Proc. Natl. Acad. Sci. U. S. A 106 (33), 14108–14113. https://doi.org/10.1073/pnas.0804650106.

Bartel, D.L., 2012. Glial responses after chorda tympani nerve injury. J. Comp. Neurol. 520 (12), 2712–2729. https://doi.org/10.1002/cne.23069.

Bartel, D.L., Finger, T.E., 2013. Reactive microglia after taste nerve injury: comparison to nerve injury models of chronic pain. F1000Research 2. https://doi.org/10.12688/f1000research.2-65.v1.

Burda, J.E., Bernstein, A.M., Sofroniew, M.V., 2016. Astrocyte roles in traumatic brain injury. Exp. Neurol. 275 (3), 305–315. https://doi.org/10.1016/j.expneurol.2015.03.020.

Bylicky, M.A., Mueller, G.P., Day, R.M., 2018. Mechanisms of endogenous neuroprotective effects of astrocytes in brain injury. Oxid. Med. Cell. Longev. https://doi.org/10.1155/2018/6501031, 2018.

Cherry, J.D., Olschowka, J.A., O'Banion, M.K., 2014. Neuroinflammation and M2 microglia: the good, the bad, and the inflamed. J. Neuroinflammation 11 (98). https://doi.org/10.1186/1742-2094-11-98.

Crain, J.M., Nikodemova, M., Watters, J.J., 2013. Microglia express distinct M1 and M2 phenotypic markers in the postnatal and adult central nervous system in male and female mice. J. Neurosci. Res. 91 (9), 1143–1151. https://doi.org/10.1002/jnr.23242.

Corson, S.L., Hill, D.L., 2011. Chorda tympani nerve terminal field maturation and maintenance is severely altered following changes to gustatory nerve input to the nucleus of the solitary tract. J. Neurosci. 31 (21), 7491–7603. https://doi.org/10.1523/JNEUROSCI.015111.2011.

Elmore, M.R.P., Hohsfield, L.A., Kramár, E.A., Soreq, L., Lee, R.J., Pham, S.T., Najafi, A.R., Spangenberg, E.E., Wood, M.A., West, B.L., Green, K.N., 2018. Replacement of microglia in the aged brain reverses cognitive, synaptic, and neuronal deficits in mice. Aging Cell 17 (6), e12832. https://doi.org/10.1111/acel.12832.

Elmore, M.R., Lee, R.J., West, B.L., Green, K.N., 2015. Characterizing newly repopulated microglia in the adult mouse: impacts on animal behavior, cell morphology, and neuroinflammation. PLoS One 10 (4), e0122912. https://doi.org/10.1371/journal.pone.0122912.

Elmore, M.R.P., Najafi, A.R., Koike, M.A., Dagher, N.N., Spangenberg, E.E., Rice, R.A., Kitazawa, M., Matusow, B., Nguyen, H., West, B.L., Green, K.N., 2014. Colony-stimulating factor 1 receptor signaling is necessary for microglia viability, unmasking a microglia progenitor cell in the adult brain. Neuron 82 (2), 380–397. https://doi.org/10.1016/j.neuron.2014.02.040.

Feng, X., Valdearcos, M., Uchida, Y., Lutrin, D., Maze, M., Koliwad, S.K., 2017. Microglia mediate postoperative hippocampal inflammation and cognitive decline in mice. JCI Insight 2 (7), e91229. https://doi.org/10.1172/jci.insight.91229.

Gao, Z., Zhu, Q., Zhang, Y., Zhao, Y., Cai, L., Shields, C.B., Cai, J., 2013. Reciprocal modulation between microglia and astrocyte in reactive gliosis following the CNS injury. Mol. Neurobiol. 48 (3), 690–701. https://doi.org/10.1007/s12035-013-8460-4.

Ginhoux, F., Greter, M., Leboeuf, M., Nandi, S., See, P., Gokhan, S., Mehler, M.F., Conway, S.J., Ng, L.G., Stanley, E.R., Samokhvalov, I.M., Merad, M., 2010. Fate mapping analysis reveals that adult microglia derive from primitive macrophages. Science 330 (6005), 841–845. https://doi.org/10.1126/science.1194637.

Goranova, V., Sifringer, M., Endesfelder, S., Ikonomidou, C., 2015. Neuroinflammation after traumatic injury to the developing brain. Scripta Sci.Med. 47 (1), 47–52.

Goranova, V., Sifringer, M., Ikonomidou, C., 2009. Activation of inflammatory mediators, microglia and astrocytes after experimental trauma to the immature rat brain. J. Biomed. Clin. Res. 2, 82–89. https://doi.org/10.3389/fped.2014.00144.

Graeber, M.B., López-Redondo, F., Ikoma, E., Ishikawa, M., Imai, Y., Nakajima, K., Kreutzberg, G.W., Kohsaka, S., 1998. The microglia/macrophage response in the neonatal rat facial nucleus following axotomy. Brain Res. 813, 241–253. https://doi.org/10.1016/S00068993(98)00859-2.

Guagliardo, N.A., Hill, D.L., 2007. Fungiform taste bud degeneration in C57BL/6J mice following chorda-lingual nerve transection. J. Comp. Neurol. 504 (2), 206–216. https://doi.org/10.1002/cne.21436.

Hammond, T.R., Dufort, C., Dissing-Olesen, L., Giera, S., Young, A., Wysoker, A., Walker, A.J., Gergits, F., Segel, M., Nemesh, J., Marsh, S.E., Saunders, A., Macosko, E., Ginhoux, F., Chen, J., Franklin, R.J.M., Piao, X., McCarroll, S.A., Stevens, B., 2019. Single-cell RNA sequencing of microglia throughout the mouse

lifespan and in the injured brain reveals complex cell-state changes. Immunity 50 (1), 253–271. https://doi.org/10.1016/j.immuni.2018.11.004.
Han, Z., Li, Q., Lan, X., EL-Mufti, L., Ren, H., Wang, J., 2019. Microglial depletion with clodronate liposomes increases proinflammatory cytokine levels, induces astrocyte activation, and damages blood vessel integrity. Mol. Neurobiol. https://doi.org/10.1007/s12035-019-1502-9.
Han, J., Zhu, K., Zhang, X.M., Harris, R.A., 2018. Enforced microglial depletion and repopulation as a promising strategy for the treatment of neurological disorders. Glia 67 (2), 217–231. https://doi.org/10.1002/glia.23529.
Heneka, M.T., Golenbock, D.T., Latz, E., 2015. Innate immunity in Alzheimer's disease. Nat. Immunol. 16 (3), 229–236. https://doi.org/10.1038/ni.3102.
Hilla, A.M., Diekmann, H., Fischer, D., 2017. Microglia are irrelevant for neuronal degeneration and axon regeneration after acute injury. J. Neurosci. 37 (25), 6113–6124. https://doi.org/10.1523/JNEUROSCI.0584-17.2017.
Himes, B.T., Tessler, A., 1989. Death of some dorsal root ganglion neurons and plasticity of others following sciatic nerve section in adult and neonatal rats. J. Comp. Neurol. 284 (2), 215–230. https://doi.org/10.1002/cne.902840206.
Hu, P., Bembrick, A.L., Keay, K.A., McLachlan, E.M., 2007. Immune cell involvement in dorsal root ganglia and spinal cord after chronic constriction or transection of the rat sciatic nerve. Brain Behav. Immun. 21 (5), 599–616. https://doi.org/10.1016/j.bbi.2006.10.013.
Imai, Y., Ibata, I., Ito, D., Ohsawa, K., Kohsaka, S., 1996. A novel gene iba1 in the major histocompatibility complex class III region encoding an EF hand protein expressed in a monocytic lineage. Biochem. Biophys. Res. Commun. 224 (3), 855–862. https://doi.org/10.1006/bbrc.1996.1112.
Ito, D., Imai, Y., Ohsawa, K., Nakajima, K., Fukuuchi, Y., Kohsaka, S., 1998. Microglia specific localisation of a novel calcium binding protein, Iba1. Mol. Brain Res. 57 (1), 1–9.
Kolb, B., Holmes, C., Whishaw, I.Q., 1987. Recovery from early cortical lesions in rats. III. Neonatal removal of posterior parietal cortex has greater behavioral and anatomical effects than similar removals in adulthood. Behav. Brain Res. 26 (2–3), 119–137.
Kopka, S.L., Geran, L.C., Spector, A.C., 2000. Functional status of the regenerated chorda tympani nerve as assessed in a salt taste discrimination task. Am. J. Physiol. Regul. Integr. Comp. Physiol. 278 (3), R720–R731. https://doi.org/10.1152/ajpregu.2000.278.3.R720.
Lee, S., Shi, X.Q., Fan, A., West, B., Zhang, J., 2018. Targeting macrophage and microglia activation with colony stimulating factor 1 receptor inhibitor is an effective strategy to treat injury-triggered neuropathic pain. Mol. Pain 14, 1–12. https://doi.org/10.1177/1744806918764979.
Li, Q., Cheng, Z., Zhou, L., Darmanis, S., Neff, N.F., Okamotom, J., Gulati, G., Bennett, M.L., Sun, L.O., Clarke, L.E., Marschallinger, J., Yu, G., Quake, S.R., Wyss-Coray, T., Barres, B.A., 2019. Developmental heterogeneity of microglia and brain myeloid cells revealed by deep single- cell RNA sequencing. Neuron 101 (2), 207–223. https://doi.org/10.1016/j.neuron.2018.12.006.
Li, Y., Yang, J., Huang, Y., Ren, D., Chi, F., 2015. Shrinkage of ipsilateral taste buds and hyperplasia of contralateral taste buds following chorda tympani nerve transection. Neural. Regen. Res. 10 (6), 989–995. https://doi.org/10.4103/1673-5374.158366.
Liddelow, S.A., Guttenplan, K.A., Clarke, L.E., Bennett, F.C., Bohlen, C.J., Schirmer, L., Bennett, M.L., Münch, A.E., Chung, W.K., Peterson, T.C., Wilton, D.K., Frouin, A., Napier, B.A., Panicker, N., Kumar, M., Buckwalter, M.S., Rowitch, D.H., Dawson, V.L., Dawson, T.M., Stevens, B., Barres, B.A., 2017. Neurotoxic reactive astrocytes are induced by activated microglia. Nature 541 (7638), 481–487. https://doi.org/10.1038/nature21029.
Martin, L.J., Lane, A.H., Samson, K.K., Sollars, S.I., 2019. Regenerative failure following rat neonatal chorda tympani transection is associated with geniculate ganglion cell loss and terminal field plasticity in the nucleus of the solitary tract. Neuroscience 402, 66–77. https://doi.org/10.1016/j.neuroscience.2019.01.011.
Martin, L.J., Sollars, S.I., 2015. Long-term alterations in peripheral taste responses to NaCl in adult rats following neonatal chorda tympani transection. Chem. Senses 40 (2), 97–108. https://doi.org/10.1093/chemse/bju063.
Melzer, P., Savchenko, V., McKanna, J.A., 2001. Microglia, astrocytes, and macrophages react differentially to central and peripheral lesions in the developing and mature rat whisker-to-barrel pathway: a study using immunohistochemistry for lipocortin 1, phosphotyrosine, s100b, and mannose receptors. Exp. Neurol. 168 (1), 63–77. https://doi.org/10.1006/exnr.2000.7554.
Morizawa, Y.M., Hirayama, Y., Ohno, N., Shibata, S., Shigetomi, E., Sui, Y., Nabekura, J., Sato, K., Okajima, F., Takebayashi, H., Okano, H., Koizumi, S., 2018. Reactive astrocytes function as phagocytes after brain ischemia via ABCA1-mediated pathway. Nat. Commun. 8 https://doi.org/10.4062/biomolther.2017.133.
Nikodemova, M., Kimyon, R.S., De, I., Small, A.L., Collier, L.S., Watters, J.J., 2015. Microglial numbers attain adult levels after undergoing a rapid decrease in cell number in the third postnatal week. J. Neuroimmunol. 278, 280–288. https://doi.org/10.1016/j.jneuroim.2014.11.018.
Okunukia, Y., Mukaia, R., Nakaob, T., Tabora, S.J., Butovskyc, O., Danab, R., Ksanderb, B.R., Connora, K.M., 2019. Retinal microglia initiate neuroinflammation in ocular autoimmunity. Proc. Natl. Acad. Sci. https://doi.org/10.1073/pnas.1820387116.
Olsson, B., Ridell, B., Jernås, M., Wadenvik, H., 2012. Increased number of B-cells in the red pulp of the spleen in ITP. Ann. Hematol. 91 (2), 271–277. https://doi.org/10.1007/s00277-0111292-2.
Omelian, J.M., Berry, M.J., Gomez, A.M., Apa, K.L., Sollars, S.I., 2016. Developmental time course of peripheral cross-modal sensory interaction of the trigeminal and gustatory systems. Dev. Neurobiol. 76 (6), 626–641. https://doi.org/10.1002/dneu.22349.
Pekny, M., Pekna, M., 2014. Astrocyte reactivity and reactive astrogliosis: costs and benefits. Physiol. Rev. 94 (4), 1077–1098. https://doi.org/10.1152/physrev.00041.2013.
Reddaway, R.B., Davidow, A.W., Deal, S.L., Hill, D.L., 2012. Impact of chorda tympani nerve injury on cell survival, axon maintenance, and morphology of the chorda tympani nerve terminal field in the nucleus of the solitary tract. J. Comp. Neurol. 520 (11), 2395–2413. https://doi.org/10.1002/cne.23044.
Rice, R.A., Spangenberg, E.E., Yamate-Morgan, H., Lee, R.J., Arora, R.P., Hernandez, M.X., Tenner, A.J., West, B.L., Green, K.N., 2015. Elimination of microglia improves functional outcomes following extensive neuronal loss in the hippocampus. J. Neurosci. 35 (27), 9977–9989. https://doi.org/10.1523/JNEUROSCI.0336-15.2015.
Riquier, A.J., Sollars, S.I., 2017. Microglia density decreases in the rat rostral nucleus of the solitary tract across development and increases in an age-dependent manner following denervation. Neuroscience 355, 36–48. https://doi.org/10.1016/j.neuroscience.2017.04.037.
Rosin, J.M., Vora, S.R., Kurraschabc, D.M., 2018. Depletion of embryonic microglia using the CSF1R inhibitor PLX5622 has adverse sex-specific effects on mice, including accelerated weight gain, hyperactivity and anxiolytic-like behavior. Brain Behav. Immun. 73, 682–697.
Shinozaki, Y., Shibata, K., Yoshida, K., Shigetomi, E., Gachet, C., Ikenaka, K., Tanaka, K.F., Koizumi, S., 2017. Transformation of astrocytes to a neuroprotective phenotype by microglia via P2Y1 receptor downregulation. Cell Rep. 19 (6), 1151–1164. https://doi.org/10.1016/j.celrep.2017.04.047.
Smith, P.L., Hagberg, H., Naylor, A.S., Mallard, C., 2014. Neonatal peripheral immune challenge activates microglia and inhibits neurogenesis in the developing murine hippocampus. Dev. Neurosci. 36 (2), 119–131. https://doi.org/10.1159/000359950.
Sofroniew, M.V., 2014. Multiple roles for astrocytes as effectors of cytokines and inflammatory mediators. The Neuroscientist 20 (2), 160–172. https://doi.org/10.1177/1073858413504466.
Sofroniew, M.V., Vinters, H.V., 2010. Astrocytes: biology and pathology. Acta Neuropathol. 119 (1), 7–35. https://doi.org/10.1007/s00401-009-0619-8.
Sollars, S.I., 2005. Chorda tympani nerve transection at different developmental ages produces differential effects on taste bud volume and papillae morphology in the rat. J. Neurobiol. 64 (3), 310–320. https://doi.org/10.1002/neu.20140.
St John, S.J., Markison, S., Spector, A.C., 1995. Salt discriminability is related to number of regenerated taste buds after chorda tympani nerve section in rats. Am. J. Physiol. 269, R141–R153. https://doi.org/10.1152/ajpregu.1995.269.1.R141.
Stephenson, J., Nutma, E., van der Valk, P., Amor, S., 2018. Inflammation in CNS neurodegenerative diseases. Immunology 154, 204–219. https://doi.org/10.1111/imm.12922.
Suzuki, H., Oku, H., Horie, T., Morishita, S., Tonari, M., Oku, K., Okubo, A., Kida, T., Mimura, M., Fukumoto, M., Kojima, S., Takai, S., Ikeda, T., 2014. Changes in expression of aquaporin-4 and aquaporin-9 in optic nerve after crushing in rats. PLoS One 9 (12), e113694. https://doi.org/10.1371/journal.pone.0114694.
Taft, J.R., Vertes, R.P., Perry, G.W., 2005. Distribution of GFAP+ astrocytes in adult and neonatal rat brain. Int. J. Neurosci. 115, 1333–1343. https://doi.org/10.1080/00207450590934570.
Tay, T.L., Mai, D., Dautzenberg, J., Fernández-Klett, F., Lin, G., Sagar, Datta, M., Drougard, A., Stempfl, T., Ardura-Fabregat, A., Staszewski, O., Margineanu, A., Sporbert, A., Steinmetz, L.M., Pospisilik, J.A., Jung, S., Priller, J., Grün, D., Ronneberger, O., Prinz, M., 2017. A new fate mapping system reveals context-dependent random or clonal expansion of microglia. Nat. Neurosci. 20 (6), 793–803. https://doi.org/10.1038/nn.4547.
Taylor, H.G., Alden, J., 1997. Age-related differences in outcomes following childhood brain insults: an introduction and overview. J. Int. Neuropsychol. Soc. 3 (6), 555–567.
Tang, Y., Le, W., 2016. Differential roles of M1 and M2 microglia in neurodegenerative diseases. Mol. Neurobiol. 53 (2), 1181–1194. https://doi.org/10.1007/s12035-014-9070-5.
Tyzack, G.E., Sitnikov, S., Barson, D., Adams-Carr, K.L., Lau, N.K., Kwok, J.C., Zhao, C., Franklin, R.J., Karadottir, R.T., Fawcett, J.W., Lakatos, A., 2014. Astrocyte response to motor neuron injury promotes structural synaptic plasticity via STAT3-regulated TSP-1 expression. Nat. Commun. 5 https://doi.org/10.1038/ncomms5294.
Villablanca, J.R., Burgess, J.W., Olmstead, C.E., 1986. Recovery of function after neonatal or adult hemispherectomy in cats: I. Time course, movement, posture and sensorimotor tests. Behav. Brain Res. 19 (3), 205–226.
Waisman, A., Ginhoux, F., Greter, M., Bruttger, J., 2015. Homeostasis of microglia in the adult brain: review of novel microglia depletion systems. Trends Immunol. 36 (10), 625–636. https://doi.org/10.1016/j.it.2015.08.005.
Wall, P.L., McCluskey, L.P., 2008. Rapid changes in gustatory function induced by contralateral nerve injury and sodium depletion. Chem. Senses 33 (2), 125–135. https://doi.org/10.1093/chemse/bjm071.
Whitehead, M.C., McGlathery, S.T., Manion, B.G., 1995. Transganglionic degeneration in the gustatory system consequent to chorda tympani damage. Exp. Neurol. 132 (2), 239–250. https://doi.org/10.1016/0014-4886(95)90029-2.
Zabel, M.K., Zhao, L., Zhang, Y., Gonzalez, S.R., Ma, W., Wang, X., Fariss, R.N., Wong, W.T., 2016. Microglial phagocytosis and activation underlying photoreceptor degeneration is regulated by CX3CL1-CX3CR1 signaling in a mouse model of retinitis pigmentosa. Glia 64 (9), 1479–1491. https://doi.org/10.1002/glia.23016.